Polyhedron 27 (2008) 2943–2951

Contents lists available at ScienceDirect

Polyhedron

journal homepage: www.elsevier.com/locate/poly

1-(2′-Pyridylazo)-2-naphtholate complexes of ruthenium: Synthesis, characterization, and DNA binding properties

Semanti Basu [a], Sarmistha Halder [a], Indrani Pal [a], Saheli Samanta [b], Parimal Karmakar [b], Michael G.B. Drew [c], Samaresh Bhattacharya [a,*]

[a] Department of Chemistry, Inorganic Chemistry Section, Jadavpur University, Raja S. C. Mullick Road, Kolkata, West Bengal 700 032, India
[b] Department of Life Science and Biotechnology, Jadavpur University, Kolkata 700 032, India
[c] Department of Chemistry, University of Reading, Whiteknights, Reading RG6 6AD, UK

ARTICLE INFO

Article history:
Received 18 January 2008
Accepted 22 May 2008
Available online 1 July 2008

Keywords:
1-(2′-Pyridylazo)-2-naphthol
Ruthenium complexes
DNA binding properties

ABSTRACT

Reaction of 1-(2′-pyridylazo)-2-naphthol (Hpan) with $[Ru(dmso)_4Cl_2]$ (dmso = dimethylsulfoxide), $[Ru(trpy)Cl_3]$ (trpy = 2,2′,2″-terpyridine), $[Ru(bpy)Cl_3]$ (bpy = 2,2′-bipyridine) and $[Ru(PPh_3)_3Cl_2]$ in refluxing ethanol in the presence of a base (NEt_3) affords, respectively, the $[Ru(pan)_2]$, $[Ru(trpy)(pan)]^+$ (isolated as perchlorate salt), [Ru(bpy)(pan)Cl] and $[Ru(PPh_3)_2(pan)Cl]$ complexes. Structures of these four complexes have been determined by X-ray crystallography. In each of these complexes, the pan ligand is coordinated to the metal center as a monoanionic tridentate N,N,O-donor. Reaction of the [Ru(bpy)(pan)Cl] complex with pyridine (py) and 4-picoline (pic) in the presence of silver ion has yielded the $[Ru(bpy)(pan)(py)]^+$ and $[Ru(bpy)(pan)(pic)]^+$ complexes (isolated as perchlorate salts), respectively. All the complexes are diamagnetic (low-spin d^6, $S = 0$) and show characteristic ^1H NMR signals and intense MLCT transitions in the visible region. Cyclic voltammetry on all the complexes shows a Ru(II)–Ru(III) oxidation on the positive side of SCE. Except in the $[Ru(pan)_2]$ complex, a second oxidative response has been observed in the other five complexes. Reductions of the coordinated ligands have also been observed on the negative side of SCE. The $[Ru(trpy)(pan)]ClO_4$, $[Ru(bpy)(pan)(py)]ClO_4$ and $[Ru(bpy)(pan)(pic)]ClO_4$ complexes have been observed to bind to DNA, but they have not been able to cleave super-coiled DNA on UV irradiation.

1. Introduction

The chemistry of ruthenium has been attracting considerable current interest [1], largely because of the fascinating photochemical, photophysical and redox properties exhibited by complexes of this metal. As all these properties are primarily directed by the coordination environment around the metal center, complexation of ruthenium by ligands of selected types is of significant importance, and the present study has originated from our interest in this area [2]. Herein we have selected 1-(2′-pyridylazo)-2-naphthol (**1**) as the principal ligand, which has been abbreviated as Hpan, where H stands for the potentially dissociable phenolic proton. This ligand is known to bind to metal centers, via dissociation of the acidic proton, as a tridentate N,N,O-donor forming two adjacent five-membered chelate rings (**2**) [3]. It is interesting to note that out of the three donor atoms, the pyridine-nitrogen as well as the azo-nitrogen are soft in nature and hence stabilize ruthenium(II) [4], while the phenolate-oxygen is hard in nature and is a recognized stabilizer of higher oxidation states of ruthenium [5]. Therefore coordination of ruthenium by ligand (**1**) is expected to impart interesting redox properties in the resulting complexes. The main objective of the present study has been to synthesize a series of ruthenium complexes of this selected ligand (**1**), and study their spectral and electrochemical properties. It may be relevant to mention here that though chemistry of complexes of ligand (**1**) with many other metals has been studied well [3], that with ruthenium appears to have received only marginal attention [6]. In the present work, reactions of ligand (**1**) have been carried out with four different ruthenium starting materials, which have afforded the homoleptic and three heteroleptic complexes. Two more mixed-ligand complexes have also been derived from one of the three heteroleptic complexes by further reaction. An account of the chemistry of all these complexes is presented in this paper, with special reference to their synthesis, structure and, spectral, electrochemical and DNA binding properties.

* Corresponding author. Tel.: +91 33 2414 6223; fax: +91 33 2414 6584.
E-mail address: samaresh_b@hotmail.com (S. Bhattacharya).

0277-5387/$ - see front matter © 2008 Elsevier Ltd. All rights reserved.
doi:10.1016/j.poly.2008.05.023

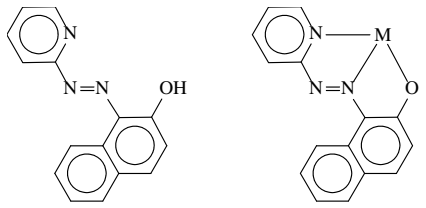

2. Experimental

2.1. Materials

Commercial ruthenium trichloride, was obtained from Arora Matthey, Kolkata, India, was converted to $RuCl_3 \cdot 3H_2O$ by repeated evaporation with concentrated hydrochloric acid. $AgNO_3$ and dimethylsulfoxide were purchased from Merck, India. Triethylamine, 2,2′-bipyridine, 2,2′,2″-terpyridine, and 1-(2′-pyridylazo)-2-naphthol (Hpan) were purchased from Loba Chemie, Mumbai, India. Pyridine and 4-picoline were purchased from Fluka Chemie. $[Ru(dmso)_4Cl_2]$, $[Ru(trpy)Cl_3]$, $[Ru(bpy)Cl_3]$ and $[Ru(PPh_3)_3Cl_2]$ were synthesized by following reported procedures [7]. Calf thymus (CT) DNA and Tris buffer were procured from Sigma Chemical Company. The dry powder of CT DNA was dissolved in 10 mM Tris buffered saline, pH 7.2 (TBS), and dialyzed overnight against the same buffer so that the A_{260}/A_{280} of the dialyzed solution was greater than 1.90. The DNA concentrations were adjusted according to its absorbance at 260 nm using $\varepsilon_{260} = 6.6\ mM^{-1}\ cm^{-1}$. SC pUC18 DNA and agarose were purchased from Bangalore Genei Pvt. Ltd., Bangalore, India. Purification of dichloromethane, acetonitrile and preparation of tetrabutylammonium perchlorate (TBAP) for electrochemical work were performed as reported in the literature [8]. All other chemicals and solvents were reagent grade commercial materials and were used as received.

2.2. Synthesis

2.2.1. $[Ru(pan)_2]$

Hpan (130 mg, 0.52 mmol) was dissolved in ethanol (50 mL) and triethylamine (55 mg, 0.54 mmol) was added to it. Then $[Ru(dmso)_4Cl_2]$ (100 mg, 0.21 mmol) was added and the mixture was refluxed for 24 h to afford a brownish-violet solution. The solvent was then evaporated and the solid mass obtained was purified by preparative thin layer chromatography on a silica plate using 1:10 acetonitrile–benzene as the eluant. A violet band separated, which was extracted with 1:1 acetonitrile–dichloromethane solution and evaporation of the extract afforded $[Ru(pan)_2]$ as a violet crystalline solid. Yield: 49 mg (40%). *Anal.* Calc. for $C_{30}H_{20}N_6O_2Ru$: C, 60.29; H, 3.35; N, 14.07. Found: C, 60.20; H, 3.39; N, 13.95%. ^1H NMR in $CDCl_3$, δ ppm[1]: 6.61 (t, 2H, $J = 6.2$); 6.85 (d, 2H, $J = 9.2$); 7.32 (d, 2H, $J = 5.3$); 7.39 (t, 4H*); 7.49 (d, 2H, $J = 9.2$); 7.64–7.73 (6H*); 10.07 (d, 2H, $J = 8.5$).

2.2.2. $[Ru(trpy)(pan)]ClO_4$

Hpan (57 mg, 0.23 mmol) was dissolved in ethanol (50 mL) and triethylamine (23 mg, 0.23 mmol) was added to it. Then $[Ru(trpy)Cl_3]$ (100 mg, 0.23 mmol) was added and the mixture was refluxed for 5 h to afford a brownish-red solution. It was then concentrated to about 10 mL, and a saturated aqueous solution of $NaClO_4$ (0.5 mL) was added, whereby a brown precipitate is obtained, which was collected by filtration, washed with cold water, and dried in vacuo over P_4O_{10}. Yield: 100 mg (65%). *Anal.* Calc. for $C_{30}H_{21}N_6O_5ClRu$: C, 52.82; H, 3.08; N, 12.32. Found: C, 52.94; H, 3.14; N, 12.25%. ^1H NMR in $CDCl_3$, δ ppm: 6.50–6.72 (2H*); 6.77 (t, 1H, $J = 6.1$); 7.2–8.0 (10H*); 8.08 (d, 2H, $J = 5.5$); 8.31 (t, 1H, $J = 8.0$); 8.47 (d, 2H, $J = 8.0$); 8.72 (d, 2H, $J = 8.0$); 10.14 (d, 1H, $J = 8.6$).

2.2.3. $[Ru(bpy)(pan)Cl]$

Hpan (70 mg, 0.28 mmol) was dissolved in ethanol (30 mL) and to it was added triethylamine (50 mg, 0.50 mmol). Then $[Ru(bpy)Cl_3]$ (100 mg, 0.28 mmol) was added to the mixture and it was refluxed for 6 h to afford a brown solution. The solvent was then evaporated and the solid mass obtained was purified by preparative thin layer chromatography on a silica plate using 1:5 acetonitrile–benzene as the eluant. A brown band separated, which was extracted with acetonitrile and evaporation of the extract afforded $[Ru(bpy)(pan)Cl]$ as a green crystalline solid. Yield: 104 mg (70%). *Anal.* Calc. for $C_{25}H_{18}N_5OClRu$: C, 55.49; H, 3.33; N, 12.95. Found: C, 55.42; H, 3.39; N, 13.02%. ^1H NMR in $CDCl_3$, δ ppm: 6.65 (t, 1H, $J = 6.4$); 6.78 (d, 1H, $J = 4.8$); 6.85 (d, 1H, $J = 9.2$); 7.00 (t, 1H, $J = 6.5$); 7.26–7.41 (2H*); 7.40 (d, 1H, $J = 9.2$); 7.53 (t, 1H, $J = 7.5$); 7.61–7.65 (2H*); 7.70 (d, 1H, $J = 8.4$); 7.80 (t, 1H, $J = 6.6$); 8.00 (t, 2H, $J = 6.9$); 8.30 (d, 1H, $J = 8.1$); 8.47 (d, 1H, $J = 5.7$); 10.07 (d, 1H, $J = 8.5$); 10.46 (d, 1H, $J = 5.7$).

2.2.4. $[Ru(bpy)(pan)(py)]ClO_4$

To a solution of $[Ru(bpy)(pan)Cl]$ (100 mg, 0.19 mmol) in ethanol (30 mL) was added $AgNO_3$ (31 mg, 0.19 mmol). The mixture was warmed and stirred for 30 min, and the deposited AgCl was separated by filtration. To the filtrate was added pyridine (15 mg, 0.19 mmol). The resulting solution was heated at reflux for 4 h. It was then concentrated to about 10 mL, and a saturated aqueous solution of $NaClO_4$ (0.5 mL) was added, whereby a reddish-brown precipitate is obtained, which was collected by filtration, washed with water, and dried in vacuo over P_4O_{10}. It was further purified by preparative thin layer chromatography on a silica plate. Using 1:5 acetonitrile–benzene as the eluant, a reddish-brown band separated, which was extracted with acetonitrile. Evaporation of this extract gave $[Ru(bpy)(pan)(py)]ClO_4$ as a crystalline solid. Yield: 76 mg (60%). *Anal.* Calc. $C_{30}H_{23}N_6O_5ClRu$: C, 52.66; H, 3.36; N, 12.29. Found: C, 51.97; H, 3.41; N, 12.34. ^1H NMR in $CDCl_3$, δ ppm: 6.81 (d, 2H, $J = 9.2$); 7.09 (t, 1H, $J = 6.3$); 7.19–7.26 (3H*); 7.40 (t, 3H*); 7.51 (d, 1H, $J = 9.3$); 7.60–7.70 (3H*); 7.72–7.81 (4H*); 8.18 (t, 1H, $J = 7.7$); 8.25–8.41 (3H*), 8.57 (d, 1H, $J = 8.0$); 9.82 (d, 1H, $J = 8.4$).

2.2.5. $[Ru(bpy)(pan)(4\text{-}pic)]ClO_4$

This complex was synthesized by following the same above procedure using 4-picoline instead of pyridine. Yield: 77 mg 60%. *Anal.* Calc. for $C_{31}H_{25}N_6O_5ClRu$: C, 53.32; H, 3.58; N, 12.04. Found: C, 53.23; H, 3.49; N, 12.10%. ^1H NMR in $CDCl_3$: δ ppm: 2.38 (s, 3H, CH_3); 6.82 (d, 1H, $J = 9.2$); 7.10 (t, 1H, $J = 6.2$); 7.15–7.20 (4H*); 7.37 (t, 1H, $J = 7.5$); 7.51 (d, 1H, $J = 9.2$); 7.55–7.85 (6H*); 8.00–8.12 (2H*); 8.18 (t, 1H, $J = 7.7$); 8.29–8.24 (3H*), 8.56 (d, 1H, $J = 8.1$); 9.83 (d, 1H, $J = 8.4$).

2.2.6. $[Ru(PPh_3)_2(pan)Cl]$

Hpan (26 mg, 0.10 mmol) was dissolved in ethanol (30 mL) and to it was added triethylamine (10 mg, 0.10 mmol). Then $[Ru(PPh_3)_3Cl_2]$ (100 mg, 0.10 mmol) was added to the solution and it was refluxed for 4 h. The $[Ru(PPh_3)_2(pan)Cl]$ complex separated as a brown precipitate, which was collected by filtration, washed with hexane and dried in air. Yield: 70 mg (74%). *Anal.* Calc. for $C_{51}H_{40}N_3OP_2ClRu$: C, 67.36; H, 4.40; N, 4.62. Found: C, 67.25; H,

[1] Chemical shifts are given in ppm and multiplicity of the signals along with the associated coupling constants (J in Hz) are given in parentheses. Overlapping signals are marked with an asterisk.

4.43; N, 4.66%. ^{1}H NMR in $CDCl_3$, δ ppm: 6.29–6.39 (2H*); 6.7–7.5 (36H*); 7.74 (d, 1H, J = 5.4); 9.20 (d, 1H, J = 8.5). ^{31}P NMR in $CDCl_3$, δ ppm: 24.14.

2.3. Physical measurements

Microanalyses (C, H, N) were performed using a Heraeus Carlo Erba 1108 elemental analyzer. Magnetic susceptibilities were measured using a PAR 155 vibrating sample magnetometer fitted with a Walker Scientific L75FBAL magnet. ^{1}H NMR spectra were recorded in $CDCl_3$ solution on a Bruker Avance DPX 300 NMR spectrometer using TMS as the internal standard. ESR spectra were recorded with a JEOL JES-FA200 X-band spectrometer fitted with a quartz Dewar for measurements at 77 K (liquid dinitrogen). All ESR spectra were calibrated with an aid of DPPH (g = 2.0037). IR spectra were obtained on a Shimadzu FTIR-8300 spectrometer with samples prepared as KBR pellets. Electronic spectra were recorded on JASCO V-570 and Shimadzu 2401 spectrophotometers. Electrochemical measurements were made using a CH Instruments model 600A electrochemical analyzer. A platinum disc working electrode, a platinum wire auxiliary electrode and an aqueous saturated calomel reference electrode (SCE) were used in the cyclic voltammetry experiments. All electrochemical experiments were performed under a dinitrogen atmosphere. All electrochemical data were collected at 298 K and are uncorrected for junction potential. Fluorescence studies were performed with a Hitachi F4500 spectrofluorimeter. Electrophoresis experiments were carried out on a BIORAD electrophoretic system using TBS. The DNA binding studies were carried out as follows: (i) Fluorescence studies were performed with the complex and DNA dissolved separately in TBS, and the samples were excited at 480 nm. (ii) For the DNA–agarose gel studies, SC pUC18 DNA was incubated in the presence of different concentrations of the complexes. These solutions were monitored on agarose gel. The DNA was visualized under UV light.

2.4. X-ray crystallography

Single crystals of $[Ru(pan)_2]$ and $[Ru(PPh_3)_2(pan)Cl]$ were obtained by slow diffusion of acetonitrile into dichloromethane solutions of the complexes, followed by evaporation of the resulting solution. Single crystals of $[Ru(trpy)(pan)]ClO_4$ and [Ru(bpy)-(pan)Cl] were obtained by slow evaporation of a solution of the complex in 1:1 dichloromethane–ethanol and acetonitrile, respectively. Selected crystal data and a summary of the data collection parameters appear below, the full details are provided in Table S1. Data on the [Ru(bpy)(pan)Cl] crystal were collected on a Enraf Nonius CAD-4 diffractometer and those for the other three crystals were collected on an Oxford Diffraction X-Calibur CCD system using graphite monochromated Mo Kα radiation (λ = 0.71073 Å). For these three crystals, X-ray data reduction was carried out using the CRYSALIS program [9c]. The structures were solved by direct methods using the SHELXS-97 program [9a]. In the structure of Ru-$(pan)_2$, the data were very weak and all atoms except for Ru were refined isotropically. In the other structures, all non-hydrogen atoms were refined anisotropically. Empirical absorption corrections were carried out using the ABSPACK program [9b]. The structures were refined on F^2 using the SHELXL-97 program [9a].

Crystal data for $C_{30}H_{20}N_6O_2Ru$, M = 597.59, size 0.05 × 0.05 × 0.30 mm^3, triclinic, space group $P\bar{1}$, a = 8.774(9) Å, b = 12.685(12) Å, c = 12.883(13) Å, α = 62.69(10)°, β = 75.07(9)°, γ = 82.15(8)°, U = 1231(2) Å^3, Z = 2, D_{calc} = 1.612 g cm^{-3}, $F(000)$ = 604, λ = 0.71073 Å, T = 150 K, μ = 0.679 mm^{-1}, 7248 reflections collected, 5936 unique (R_{int} = 0.225). Final goodness-of-fit = 0.414, R_1 = 0.0701, wR_2 = 0.0878, R indices based on 630 reflections with [$I > 2\sigma(I)$].

Crystal data for $C_{30}H_{21}N_6O_5ClRu$, M = 680.03, size 0.05 × 0.10 × 0.20 mm^3, monoclinic, space group $C2/c$, a = 30.611(4) Å, b = 11.6611(14) Å, c = 16.491(2) Å, $\alpha = \gamma$ = 90°, β = 114.595(13)°, U = 5352.5(13) Å^3, Z = 8, D_{calc} = 1.688 g cm^{-3}, $F(000)$ = 2736, λ = 0.71073 Å, T = 150 K, μ = 0.741 mm^{-1}, 18729 reflections collected, 7821 unique (R_{int} = 0.109). Final goodness-of-fit = 0.615, R_1 = 0.0486, wR_2 = 0.0790, R indices based on 2125 reflections with [$I > 2\sigma(I)$].

Crystal data for $C_{25}H_{18}N_5OClRu$, M = 540.96, size 0.10 × 0.10 × 0.40 mm^3, orthorhombic, space group $P2_12_12_1$, a = 10.2654(9) Å, b = 13.2256(12) Å, c = 15.7074(14) Å, $\alpha = \beta = \gamma$ = 90°, U = 2132.5(3) Å^3, Z = 4, D_{calc} = 1.685 g cm^{-3}, $F(000)$ = 1088, λ = 0.71073 Å, T = 100 K, μ = 0.890 mm^{-1}, 14079 reflections collected, 5257 unique (R_{int} = 0.045). Final goodness-of-fit = 1.03, R_1 = 0.039, wR_2 = 0.0967, R indices based on 5257 reflections with [$I > 2\sigma(I)$].

Crystal data for $C_{52}H_{42}N_3OP_2Cl_3Ru$, M = 994.25, size 0.10 × 0.20 × 0.30 mm^3, monoclinic, spacegroup Cm, a = 18.325(3) Å, b = 15.2504(12) Å, c = 9.6397(8) Å, $\alpha = \gamma$ = 90°, β = 122.099(5)°, U = 2282.1(5) Å^3, Z = 4, D_{calc} = 1.447 g cm^{-3}, $F(000)$ = 1016, λ = 0.71073 Å, T = 150 K, μ = 0.632 mm^{-1}, 7207 reflections collected, 4280 unique (R_{int} = 0.040). Final goodness-of-fit = 1.007, R_1 = 0.0384, wR_2 = 0.0845, R indices based on 3596 reflections with [$I > 2\sigma(I)$].

3. Results and discussion

3.1. Syntheses and crystal structures

The primary objective of the present study, as already mentioned above, has been to synthesize a series of ruthenium complexes containing 1-(2′-pyridylazo)-2-naphthol (Hpan, **1**), either as the sole ligand or as one of the ligands. For preparing the homoleptic ruthenium complex of Hpan, $[Ru(dmso)_4Cl_2]$ has been selected as the starting material because of its demonstrated ability to undergo displacement of all the six monodentate ligands by chelating ligands [2j,2n]. Reaction of Hpan with $[Ru(dmso)_4Cl_2]$ in refluxing ethanol in the presence of triethylamine has indeed afforded the expected bis-complex, *viz.* $[Ru(pan)_2]$, in a decent yield (Scheme 1). In order to authenticate coordination mode of ligand (**1**) in this complex, its structure has been determined by X-ray crystallography. The structure is shown in Fig. 1 and selected bond parameters are given in Table 1.

The structure shows that in this complex 1-(2′-pyridylazo)-2-naphthol is coordinated to the metal center, via dissociation of the phenolic proton, as a monoanionic N,N,O-donor (**2**, M = Ru),

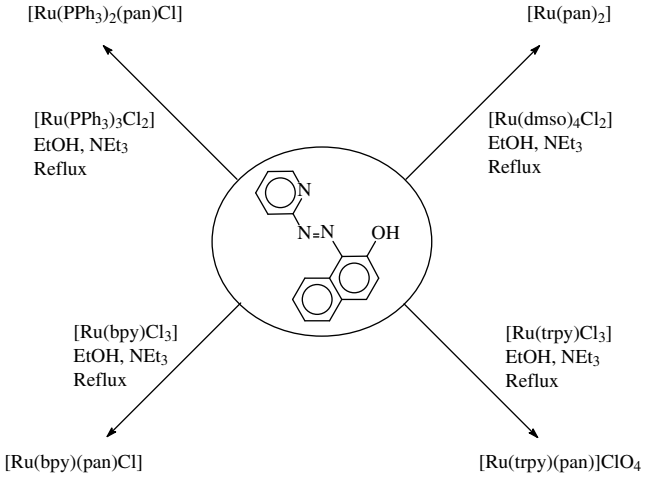

Scheme 1.

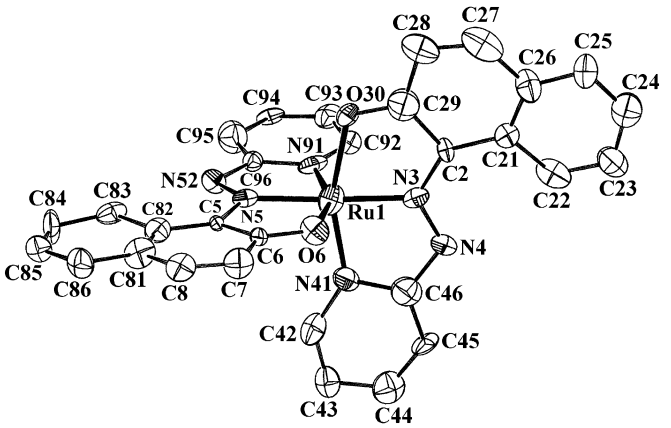

Fig. 1. View of the $[Ru(pan)_2]$ complex (ellipsoids at 25% probability, hydrogens not included for clarity).

Table 1
Selected bond lengths (Å) and bond angles (°) for $[Ru(pan)_2]$, $[Ru(trpy)(pan)]ClO_4$, [Ru(bpy)(pan)Cl] and $[Ru(PPh_3)_2(pan)Cl]$ complexes

$[Ru(pan)_2]$			
Bond distances (Å)			
Ru(1)–N(3)	1.973(10)	Ru(1)–O(6)	2.053(9)
Ru(1)–N(5)	1.965(10)	Ru(1)–O(30)	2.105(8)
Ru(1)–N(41)	1.985(11)	N(3)–N(4)	1.427(13)
Ru(1)–N(91)	2.068(10)	N(5)–N(52)	1.349(11)
Bond angles (°)			
N(3)–Ru(1)–N(5)	177.8(5)	N(3)–Ru(1)–O(30)	78.2(4)
N(41)–Ru(1)–O(30)	160.0(3)	N(5)–Ru(1)–N(91)	77.7(4)
N(91)–Ru(1)–O(6)	157.4(3)	N(5)–Ru(1)–O(6)	79.8(4)
N(3)–Ru(1)–N(41)	81.7(4)		
$[Ru(trpy)(pan)]ClO_4$			
Bond lengths (Å)			
Ru(1)–N(11)	2.049(4)	Ru(1)–N(38)	1.919(4)
Ru(1)–N(22)	1.998(4)	Ru(1)–O(52)	2.077(3)
Ru(1)–N(28)	2.058(4)	N(37)–N(38)	1.337(4)
Ru(1)–N(31)	2.032(4)		
Bond angles (°)			
N(11)–Ru(1)–N(28)	156.43(16)	N(22)–Ru(1)–N(28)	78.55(16)
N(22)–Ru(1)–N(38)	177.82(16)	N(31)–Ru(1)–N(38)	77.49(16)
N(31)–Ru(1)–O(52)	158.65(15)	N(38)–Ru(1)–O(52)	81.18(15)
N(11)–Ru(1)–N(22)	78.09(16)		
[Ru(bpy)(pan)Cl			
Bond lengths (Å)			
Ru–N(1)	1.910(3)	Ru–O	2.102(2)
Ru–N(3)	2.039(3)	Ru–Cl	2.3830(10)
Ru–N(4)	2.042(3)	O–C(1)	1.289(4)
Ru–N(5)	2.093(3)	N(1)–N(2)	1.316(4)
Bond angles (°)			
N(1)–Ru–N(5)	174.92(12)	N(1)–Ru–N(3)	79.23(12)
N(3)–Ru–O	160.94(10)	N(4)–Ru–N(5)	78.03(12)
N(4)–Ru–Cl	172.45(9)	N(1)–Ru–O	81.72(10)
$[Ru(PPh_3)_2(pan)Cl]$			
Bond lengths (Å)			
Ru(1)–N(41)	2.058(4)	Ru(1)–Cl(1)	2.4786(14)
Ru(1)–N(44)	1.916(5)	O(55)–C(54)	1.291(6)
Ru(1)–O(55)	2.130(4)	N(43)–N(44)	1.327(6)
Ru(1)–P(2)	2.3873(9)		
Bond angles (°)			
N(41)–Ru(1)–O(55)	159.50(14)	N(41)–Ru(1)–N(44)	79.5(2)
N(44)–Ru(1)–Cl(1)	173.99(15)	N(44)–Ru(1)–O(55)	80.02(17)
P(2)–Ru(1)–P(2a)	166.74(4)		

with N–Ru–N and N–Ru–O bite angles of ~79°. In this complex ruthenium is thus sitting in a N_4O_2 coordination sphere, which is significantly distorted from ideal octahedral geometry, primarily because of the strain imposed by the two adjacent five-membered chelate rings. The phenolic C–O distance is normal [2n], while the average N–N distance is notably longer than that in uncoordinated azo ligands [10] and the observed elongation is attributable to the metal-to-π^*(azo) back-bonding [11]. The absence of any solvent of crystallization in the crystal lattice of $[Ru(pan)_2]$ indicates the possible existence of non-covalent interactions between the individual complex molecules. To sort this out, packing pattern in the lattice has been examined, which shows that hydrogen-bonding interactions of two types, *viz.* C–H···O and C–H···π interactions, are active in the lattice (Fig. 2). The phenolate-oxygen of each coordinated pan of any complex molecule each coordinated pan of any complex molecule is hydrogen-bonded to two aryl hydrogens of two other pan ligands belonging to two different complex molecules. The δ-hydrogen in the azo-linked phenyl ring of the naphthol fragment of each pan is involved in a C–H···π interaction with the π-cloud over the other ring of the naphthol fragment of another pan of a second neighboring complex molecule. Both of these hydrogen-bonding interactions are extended throughout the entire lattice, and they appear to be responsible for holding the crystal together.

As 1-(2′-pyridylazo)-2-naphthol (**1**) serves as a N,N,O-donor and forms a planar chelate (**2**), in the Ru(pan) fragment only three coordination sites on ruthenium remain accessible. To occupy these three available sites either a planar tridentate ligand, or a combination of a bidentate and a monodentate ligand, or three monodentate ligands can be utilized to obtain the mixed-ligand complexes. Accordingly three different ruthenium starting materials, *viz.* $[Ru(trpy)Cl_3]$ (trpy = 2,2′,2″-terpyridine), $[Ru(bpy)Cl_3]$ (bpy = 2,2′-bipyridine) and $[Ru(PPh_3)_3Cl_2]$, have been chosen. Reactions of ligand (**1**) with these three starting materials in refluxing ethanol in the presence of triethylamine have afforded the targeted mixed-ligand complexes, *viz.* $[Ru(trpy)(pan)]^+$ (isolated as the perchlorate salt), [Ru(bpy)(pan)Cl] and $[Ru(PPh_3)_2(pan)Cl]$, respectively, in good yields (Scheme 1). It is interesting to note here that during synthetic reactions of Hpan with $[Ru(trpy)Cl_3]$ and $[Ru(bpy)Cl_3]$, ruthenium undergoes a one-electron reduction, and either the solvent (ethanol) or the base (NEt_3) might have served as the reducing agent. Structures of these three mixed-ligand complexes have also been determined by X-ray crystallography. Structure of the $[Ru(trpy)(pan)]ClO_4$ complex (Fig. 3) shows that in it the pan ligand is coordinated to ruthenium as before. The remaining three coordination sites on ruthenium are occupied by the three terpyridine-nitrogens in the usual manner. The N_5O coordination sphere around ruthenium is similarly distorted from ideal octahedral geometry as in $[Ru(pan)_2]$, because like the 1-(2′-pyridylazo)-2-naphtholate anion (pan), terpyridine also forms two adjacent five-membered chelate rings. Bond parameters (Table 1) in the Ru(trpy) fragment are found to be normal, as observed in other structurally characterized complexes of ruthenium having this fragment [12]. Bond lengths in the Ru(pan) fragment are comparable to those observed in the $[Ru(pan)_2]$ complex. An examination of the packing pattern in the lattice of the $[Ru(trpy)(pan)]ClO_4$ complex shows the existence of three types of hydrogen-bonding interactions, *viz.* C–H···O, C–H···N and C–H···π interactions (Fig. S1). Two perchlorate-oxygens are hydrogen-bonded to pyridyl-hydrogens of the terpyridine. One pyridyl-hydrogen of the terpyridine is hydrogen-bonded to an azo-nitrogen of the pan ligand of another complex molecule. The γ-hydrogen of the naphthol fragment of pan is involved in a C–H···π interaction with the π-cloud of the pyridine ring of pan of another complex molecule.

Structure of the [Ru(bpy)(pan)Cl] complex (Fig. 4) shows that the pan ligand is coordinated in the expected N,N,O-mode, while the remaining three sites are occupied by a 2,2′-bipyridine, coordinated in the usual N,N-fashion, and a chloride. The observed Ru–Cl length (Table 1) is normal, and so are the bond distances in the Ru(bpy) fragment [13]. The octahedral N_4OCl coordination sphere

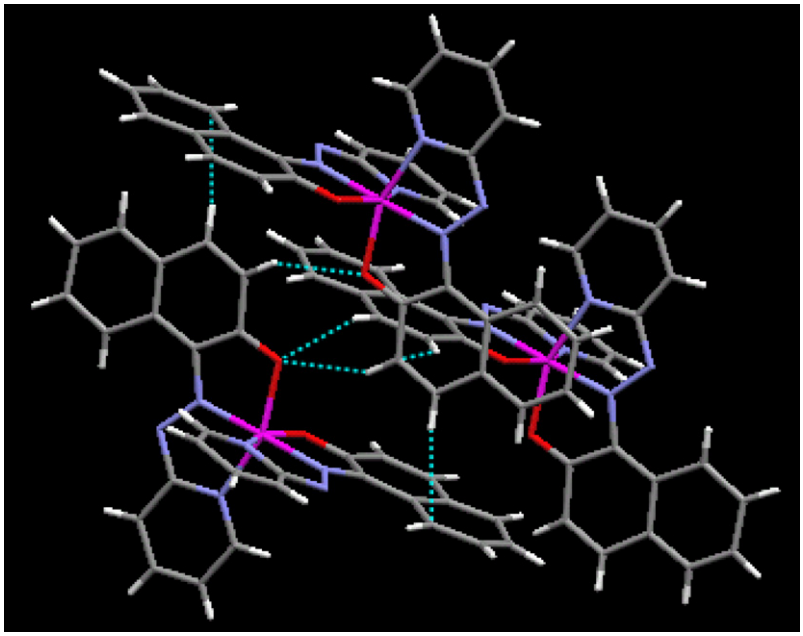

Fig. 2. Packing diagram of [Ru(pan)$_2$] complex.

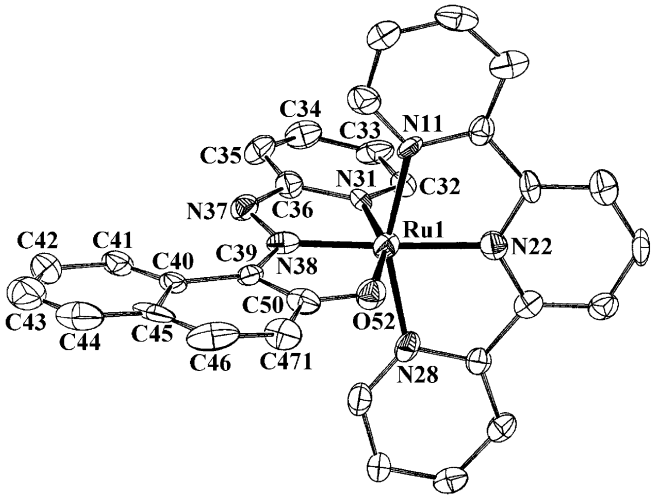

Fig. 3. View of the [Ru(trpy)(pan)]$^+$ complex (ellipsoids at 25% probability, hydrogens not included for clarity).

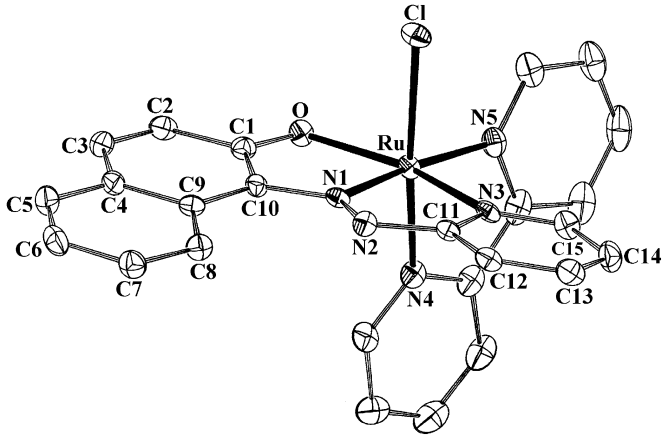

Fig. 4. View of the [Ru(bpy)(pan)Cl] complex (ellipsoids at 25% probability, hydrogens not included for clarity).

in this complex is much less distorted compared to the structures of the [Ru(pan)$_2$] and [Ru(trpy)(pan)]$^+$ complexes, because of the flexibility associated with a bidentate and a monodentate ligands replacing a tridentate ligand forming two adjacent five-membered chelate rings. An examination of the packing pattern in the lattice of the [Ru(bpy)(pan)Cl] complex shows the existence of three types of non-covalent interactions, *viz.* C–H···O, C–H···Cl and C–H···π interactions (Fig. S2). The phenolate oxygen of pan is hydrogen-bonded to a pyridyl hydrogen of bpy belonging to a neighboring complex molecule. The chloride is hydrogen-bonded to a pyridyl C–H of pan of an adjacent complex molecule. Besides these hydrogen-bonding interactions there are intermolecular C–H···π interactions between two pyridyl C–H's of the bipyridine ligand and naphthyl π-cloud. There is also a C–H···π interaction between a pyridyl C–H of pan ligand of one molecule with a pyridyl π cloud of another.

The structure of the [Ru(PPh$_3$)$_2$(pan)Cl] complex (Fig. 5) has mirror symmetry and shows the pan ligand and the chloride sharing an equatorial plane with the metal at the center, where the chloride is obviously trans to the coordinated azo nitrogen, and the two triphenylphosphines occupy the remaining two axial positions and hence they are mutually trans. Compared to the structures of the previous complexes, the N_2OP_2Cl coordination sphere in the present complex is far less distorted, which is attributable to the freedom in disposition of three monodentate ligands. The Ru–P lengths (Table 1) are normal [2i], but the Ru–Cl distance is notably longer than that observed in the [Ru(bpy)(pan)Cl] complex and the observed elongation is attributable to stronger trans effect of the azo-nitrogen than that of the bpy-nitrogen. In the crystal lattice of this complex, there exists one molecule of dichloromethane per molecule of the complex. To find out the non-covalent interaction(s) active in the lattice, particularly between the solvent molecule and the complex molecule, packing pattern in the lattice has been examined (Fig. S3), which reveals that each complex molecule is linked to four surrounding complex molecules through C–H···π interactions. The phenyl C–H of triphenylphosphine is involved in non-covalent interaction with the π cloud on both the pyridyl and naphthyl ring of pan. Each coordinated chloride is engaged in C–H···Cl hydrogen bonding with the hydrogens of the nearest dichloromethane molecule.

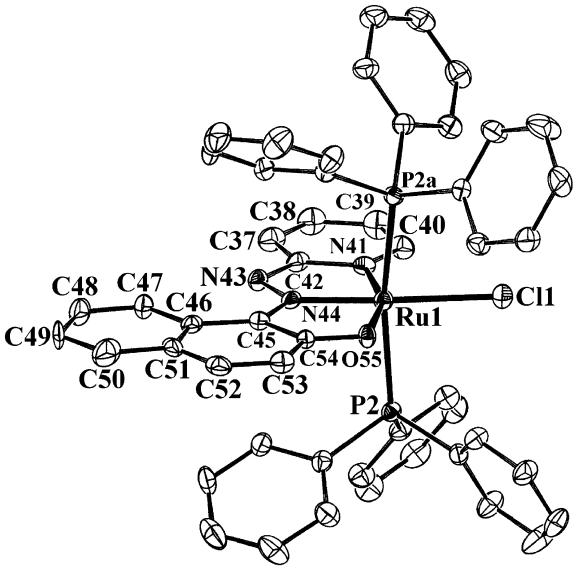

Fig. 5. View of the [Ru(PPh$_3$)$_2$(pan)Cl] complex (ellipsoids at 25% probability, hydrogens not included for clarity).

The coordinated chloride in the [Ru(bpy)(pan)Cl] complex has been found to undergo facile displacement by other monodentate ligands under relatively mild condition. This has been manifested in the reactions of [Ru(bpy)(pan)Cl] with pyridine (py) and 4-picoline (pic) carried out in ethanolic medium in the presence of silver ion, for easy removal of the coordinated chloride, which have yielded the desired mixed-ligand complexes, *viz.* [Ru(bpy)(pan)(py)]$^+$ and [Ru(bpy)(pan)(pic)]$^+$, isolated as perchlorate salts in good yields. Composition of these two complexes has been verified by their microanalytical data. Both of these complexes are assumed to have a similar structure as the precursor [Ru(bpy)(pan)Cl] complex, with the chloride replaced by pyridine or 4-picoline.

3.2. Spectral properties

All the six complexes, *viz.* [Ru(pan)$_2$], [Ru(trpy)(pan)]ClO$_4$, [Ru(bpy)(pan)Cl], [Ru(PPh$_3$)$_2$(pan)Cl], [Ru(bpy)(pan)(py)]ClO$_4$ and [Ru(bpy)(pan)(pic)]ClO$_4$, are diamagnetic, which corresponds to the bivalent state of ruthenium (low-spin d^6, $S = 0$) in them. ^{1}H NMR spectra of these complexes have been recorded in CDCl$_3$ solution and a spectrum has been deposited as supplementary material (Fig. S4). ^{1}H NMR spectrum of the [Ru(pan)$_2$] complex shows all the expected signals within 6.5–10.1 ppm, of which the most deshielded doublet at 10.07 ppm is assignable to the proton nearest to the pyridine-nitrogen. Spectra of the other three complexes are complex in nature due to overlap of signals arising from both pan and other organic ligand(s) in the similar region. However, in all these three spectra the isolated doublet near 10.0 ppm, which is diagnostic of coordinated pan, is clearly observed. ^{1}H NMR spectrum of the [Ru(bpy)(pan)(py)]ClO$_4$ complex shows most of the expected signals clearly, though few signals could not be distinctly identified due to their overlap with other signals. The methyl signal from the 4-picoline fragment of the [Ru(bpy)(pan)(pic)]ClO$_4$ complex is observed at 2.38 ppm, while rest of its ^{1}H NMR spectrum is very similar to that of the [Ru(bpy)(pan)(py)]ClO$_4$ complex.

Infrared spectra of the complexes show many bands of different intensities within 400–4000 cm^{-1}. Assignment of each individual band to a specific vibration has not been attempted. However, strong bands observed at 1606, 1498, 1199, 1134, 758 cm^{-1} in the spectrum of the [Ru(pan)$_2$] complex are assignable to the coordinated pan ligand. Such bands are also observed in the other five complexes. In the spectra of the [Ru(trpy)(pan)]ClO$_4$, [Ru(bpy)(pan)(py)]ClO$_4$ and [Ru(bpy)(pan)(pic)]ClO$_4$ complexes two intense bands are observed near 1080 and 620 cm^{-1}, which are attributed to the perchlorate ion. Infrared spectrum of [Ru(PPh$_3$)$_2$(pan)Cl] shows sharp bands at 744, 698 and 519 cm^{-1} due to the coordinated PPh$_3$ ligands.

All the complexes are found to be soluble in ethanol, methanol, acetonitrile, dichloromethane and chloroform, producing reddish-brown solutions. Electronic spectra of the complexes have been recorded in dichloromethane solution. Each complex shows several intense absorptions in the visible and ultraviolet region (Table 2). The absorptions in the ultraviolet region are believed to be due to transitions within the ligand orbitals and those in the visible region are likely to be due to allowed metal-to-ligand charge-transfer transitions. To have a better understanding of the nature of transitions in the visible region, qualitative EHMO calculations have been performed on computer-generated models[2] of all the complexes [14]. Composition of some selected molecular orbitals is given in Table S2 and partial MO diagram of the [Ru(pan)$_2$] complex is shown in Fig. 6. The top three filled orbitals, *viz.* the highest occupied molecular orbital (HOMO) and the next two filled orbitals (HOMO−1 and HOMO−2), are close in energy and have major contributions from the ruthenium t_2-orbitals and relatively less contributions from the coordinated ligands. The lowest unoccupied molecular orbital (LUMO), though has some contribution from the metal center, is localized mostly on the pan ligand and is concentrated heavily on the azo (-N=N-) fragment. The next couple of vacant orbitals (LUMO + 1, LUMO + 2, etc.) are delocalized over either pan or the co-ligand. The lowest energy absorption in the visible region may therefore be assigned to a transition between the strongly

Table 2
Electronic spectral and cyclic voltammetric data

Compound	Electronic spectral data[a] λ_{max}, nm (ε, M^{-1} cm^{-1})	Cyclic voltammetric data[b]
[Ru(pan)$_2$]	606(11240), 566[c](9370), 548[c](9240), 470(9710), 408(8040), 368(10390), 302(13020)	1.62[d], 0.70[e](80)[f], −0.94[e](89)[f]
[Ru(trpy)(pan)]ClO$_4$	548(16730), 480(24060), 456[c](16070), 376[c]10710), 318(32980), 282(28680), 272(29200), 228(47040)	1.66[d], 0.86[e](69)[f], −0.86[e](90)[f], −1.56[e](60)[f]
[Ru(bpy)(pan)Cl]	610[c](13140), 584[c](12570), 504(36050), 476(22170), 444[c](12360), 368(22290), 296(48210)	1.59[d], 0.44[e](78)[f], −0.88[e](90)[f], −1.58[g]
[Ru(PPh$_3$)$_2$(pan)Cl]	550(5560), 480(18770), 456(9610)[c], 368(12430), 307(14780)[c], 269(41870)	1.54[d], 0.47[e](67)[f], −1.00[e](96)[f]
[Ru(bpy)(pan)(py)]ClO$_4$	595[c](11250), 572(12800), 555[c](11900), 492(31500), 465(20500), 389[c](16600), 346(19200), 293(43900)	1.69[d], 0.82[e](70)[f], −0.92[e](80)[f], −1.52[g]
[Ru(bpy)(pan)(pic)]ClO$_4$	594[c](7800), 576[c](8400), 492(22100), 464(14000), 388[c](11200), 342(12500), 292(29600)	1.64[d], 0.79[e](71)[f], −0.94[e](83)[f], −1.57[g]

[a] In dichloromethane.
[b] Solvent, 1:9 dichloromethane–acetonitrile; supporting electrolyte, TBAP; reference electrode, SCE; scan rate, 50 mV s^{-1}.
[c] Shoulder.
[d] Anodic peak-potential (E_{pa}) value.
[e] $E_{1/2} = 0.5(E_{pa} + E_{pc})$, where E_{pc} = cathodic peak-potential.
[f] $\Delta E_p = (E_{pa} - E_{pc})$ in mV.
[g] E_{pc} value.

[2] In the [Ru(PPh$_3$)$_2$(pan)Cl] complex phenyl rings of the triphenylphosphines are replaced by hydrogen.

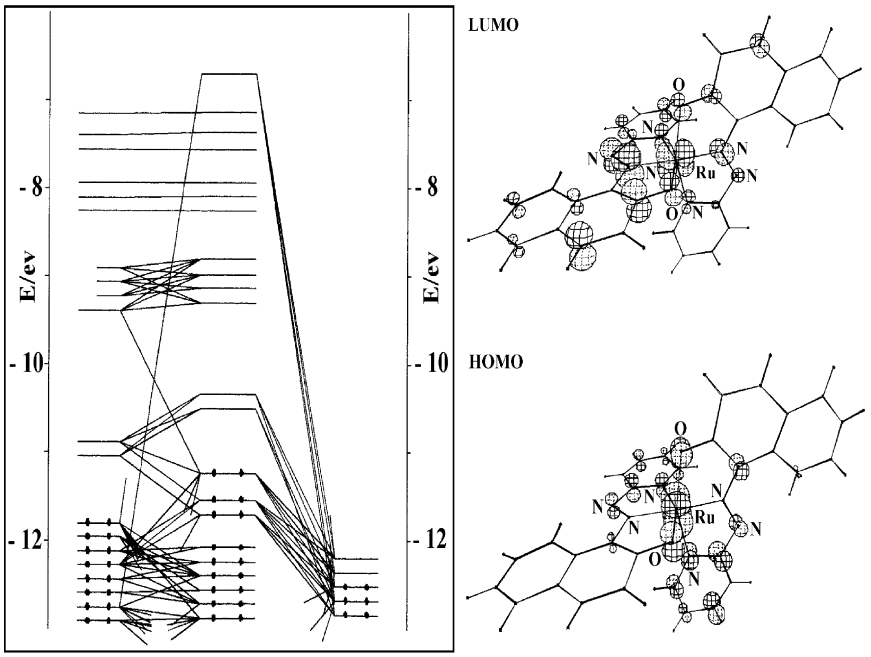

Fig. 6. Partial molecular orbital diagram of [Ru(pan)$_2$]: (a) interaction diagram and (b) highest occupied and lowest unoccupied molecular orbitals.

delocalized HOMO and LUMO with mixed metal-to-ligand charge-transfer (MLCT) and intra-ligand charge-transfer (ILCT) transition.

3.3. Electrochemical properties

Electrochemical properties of all the complexes have been studied by cyclic voltammetry in 1:9 dichloromethane–acetonitrile[3] solution (0.1 M TBAP). The voltammetric data are given in Table 2. All the complexes show two oxidative responses on the positive side of SCE. In view of the composition of the HOMO, the first oxidation is tentatively assigned to the Ru(II)–Ru(III) oxidation. This oxidation is reversible in nature, characterized by a peak-to-peak separation (ΔE_p) of 67–80 mV, which remains unchanged upon changing the scan rate, and the anodic peak-current (i_{pa}) is almost equal to the cathodic peak-current (i_{pc}) as expected for a reversible electron-transfer process. Reversibility of the Ru(II)–Ru(III) oxidation indicates that the one-electron oxidized species might be stable on a time scale much longer than the cyclic voltammetric time scale. To investigate this, as well as to verify assignment of this oxidative response to Ru(II)–Ru(III) oxidation, all the six complexes have been coulometrically oxidized at an appropriate potential[4] in 1:9 dichloromethane–acetonitrile solution (0.1 M TBAP). The oxidations have been smooth and quantitative for each complex. However, the oxidized solutions are found to stable only for the [Ru(bpy)(pan)Cl] and [Ru(PPh$_3$)$_2$(pan)Cl] complexes, which have much less Ru(II)–Ru(III) oxidation potential. For the rest four complexes, color of the solution containing the oxidized species changes rapidly indicating fast decomposition. ESR spectra of solutions containing the [Ru(bpy)(pan)Cl]$^+$ and [Ru(PPh$_3$)$_2$(pan)Cl]$^+$ complexes have been recorded at 77 K. Both the complexes show an axial ESR spectrum with two distinct signals ($g_\perp$ and $g_\parallel$; for the [Ru(bpy)-(pan)Cl]$^+$ complex $g_\perp = 2.28$ and $g_\parallel = 1.90$; for the [Ru(PPh$_3$)$_2$(pan)Cl]$^+$ complex $g_\perp = 2.21$ and $g_\parallel = 1.99$). A selected spectrum is shown in Fig. 7. The observed anisotropic nature of the spectra confirms the +3 oxidation state of ruthenium in the oxidized complexes, which in turn supports assignment of the first oxidative response to Ru(II)–Ru(III) oxidation to be correct. The second oxidative response is irreversible in nature and is tentatively assigned to oxidation of the coordinated pan ligand. A reductive response, quasi-reversible in nature, is displayed by all the complexes near −0.9 V versus SCE, and in view of the composition of the LUMO this reduction is assigned to reduction of the azo (–N=N–) fragment of the coordinated pan ligand. A second irreversible reductive response is observed in the [Ru(trpy)(pan)]ClO$_4$, [Ru(bpy)(pan)Cl],

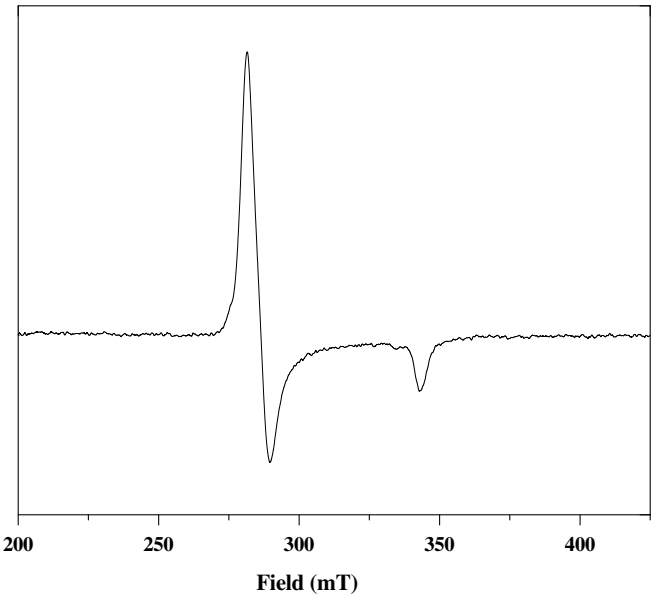

Fig. 7. ESR spectrum of the [Ru^{III}(bpy)(pan)Cl]$^+$ complex in 1:9 dicloromethane–acetonitrile solution at 77 K.

[3] A little dichloromethane was necessary to take the complex into solution. Addition of large excess of acetonitrile was necessary to record the redox responses in proper shape.

[4] Coulometric oxidation has been carried out at a potential 200 mV higher than the anodic peak-potential (E_{pa}).

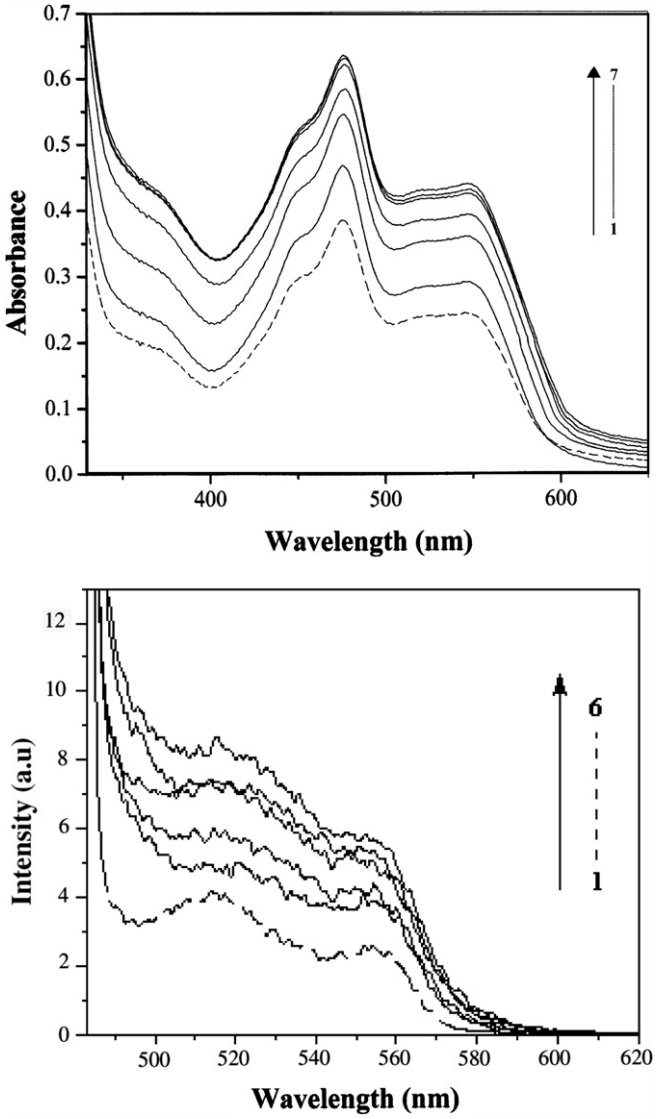

Fig. 8. (a) Absorption spectrum of the [Ru(trpy)(pan)]ClO_4 in Tris–HCl/NaCl buffer (10 mM, pH 7.2) solution in the absence (---) and presence (—) of CT DNA ([DNA]:[complex] = 20:1, 40:1, 50:1, 60:1, 65:1, 70:1; the complex concentration was 30 μM). (b) Fluorescence spectrum of the [Ru(trpy)(pan)]ClO_4 in Tris–HCl/NaCl buffer (10 mM, pH 7.2) solution in the absence (---) and presence (—) of CT DNA ($\lambda_{excitation}$ = 480 nm, [DNA]:[complex] = 40:1, 50:1, 60:1, 65:1, 70:1; the complex concentration was 30 μM).

[Ru(bpy)(pan)(py)]ClO_4 and [Ru(bpy)(pan)(pic)]ClO_4 complexes around −1.6 V versus SCE, which is assigned to reduction of the coordinated polypyridine (trpy or bpy) ligand [13].

3.4. DNA binding properties

As cationic transition metal complexes containing polypyridine ligands are known to display DNA interaction properties [15], we have also explored such possibility in the three such cationic complexes, *viz.* [Ru(trpy)(pan)]ClO_4, [Ru(bpy)(pan)(py)]ClO_4 and [Ru(bpy)(pan)(pic)]ClO_4. These three complexes are fairly soluble in water, another property welcome in DNA binding agents. Interaction of the [Ru(trpy)(pan)]ClO_4 complex with DNA has been monitored initially by absorption and fluorescence spectroscopic studies in Tris–HCl buffer (pH 7.2) solution. In the absorption spectroscopic studies, the maximum at 480 nm, displayed by the complex only, is found to increase in intensity upon addition of DNA. The intensity increases with increasing ratio of [DNA]:[complex] and reaches saturation at [DNA]:[complex] = 70:1 (Fig. 8a). Such increase in intensity of absorption upon interaction with DNA is, though relatively less common, precedent in the literature [16]. In order to explore the interaction one step further, detailed spectrofluorimetric experiments with complex and DNA has also been carried out. The complex shows emission peaks at 515 nm and 554 nm when excited at 480 nm. With the increasing amount of DNA the fluorescence intensity increases for both the peaks (Fig. 8b), and reaches its optimum value in the same ratio (i.e. [DNA]:[complex] = 70:1). Absorption and fluorescence spectroscopic studies in Tris–HCl buffer (pH 7.2) solution in the presence and absence of DNA show that the other two complexes, *viz.* [Ru(bpy)(pan)(py)]ClO_4 and [Ru(bpy)(pan)(pic)]ClO_4, also interact with DNA.

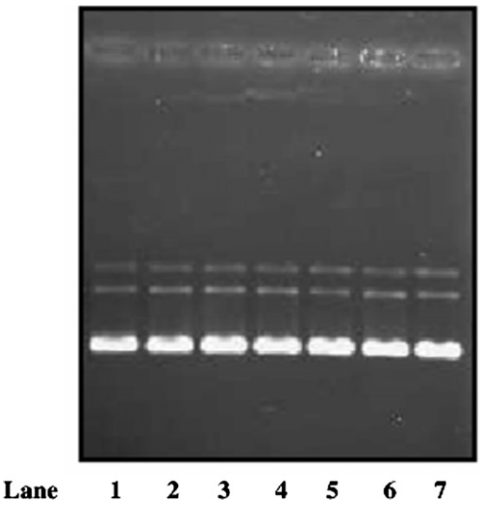

Fig. 9. Results of the gel electrophoresis experiment for [Ru(trpy)(pan)]ClO_4. Lane 1, SC pUC18 DNA control without irradiation. Lane 2, DNA control with irradiation at 254 nm. Lanes 3–7, DNA + complex with [DNA]/[complex] ratio of 1, 20, 40, 60, 70, respectively with irradiation at 254 nm. The complex concentration was 30 μM for Lanes 3–7.

In order to examine whether the above three complexes can also bring about cleavage of DNA upon UV irradiation, a property usually exhibited by such polypyridine complexes [15], interaction of these complexes with a super-coiled DNA, *viz.* SC pUC18 DNA, has been studied by gel electrophoresis. In these experiments SC pUC18 DNA was incubated in the presence of different concentrations of the complexes, followed by irradiation at 254 nm for different time durations. The samples were then analyzed by agarose gel electrophoresis. After the run the DNA was stained with EtBr and visualized by UV transilluminator. A representative picture of EtBr stained DNA is shown in Fig. 9. The extreme left line is for SC pUC18 DNA and in the following five lanes are the bands for increasing DNA complex ratio (i.e. [DNA]/[complex] = 1, 20, 40, 60 and 70. This shows that the complex does not induce any observable conformation changes in SC DNA confirming that they cannot cleave DNA upon UV irradiation. Moreover we could not see any retardation of the SC pUC18 DNA. This is perhaps due to the dissociation of the complex from DNA during the run of gel electrophoresis.

4. Conclusions

The present study shows that 1-(2′-pyridylazo)-2-naphthol (Hpan) can bind strongly to ruthenium as a monoanionic N,N,O-donor affording stable complexes. The mixed-ligand [Ru(bpy)(pan)Cl] complex exhibits interesting reactivity via dissociation of the Ru–Cl bond and such reactions with different bridging and

terminal ligands are currently under exploration. The [Ru(trpy)(pan)]ClO_4, [Ru(bpy)(pan)(py)]ClO_4 and [Ru(bpy)(pan)(pic)]ClO_4 complexes can effectively bind to DNA without causing damage to the DNA double helix.

Acknowledgements

The authors thank the reviewers for their critical comments, which have been useful in revising the manuscript. They also thank Prof. P.K. Bharadwaj, Department of Chemistry, Indian Institute of Technology, Kanpur, for his help with the X-ray diffraction data collection on the crystal of [Ru(bpy)(pan)Cl]. Thanks are also due to Prof. S. Pal of University of Hyderabad (for recording the esr spectra) and, Prof. K.P. Das and Mr. P. Dey of Bose Institute (for their help in recording the fluorescence spectra). Professor Michael G.B. Drew thanks the Engineering and Physical Sciences Research Council, United Kingdom and the University of Reading, for financial help. S. Halder thanks the University Grants Commission, New Delhi [Grant No. 10–2(5)2004(1)-E.U.II] for her fellowship.

Appendix A. Supplementary data

CCDC 644619 and 644622 contains the supplementary crystallographic data for this paper. These data can be obtained free of charge via http://www.ccdc.cam.ac.uk/conts/retrieving.html, or from the Cambridge Crystallographic Data Centre, 12 Union Road, Cambridge CB2 1EZ, UK; fax: (+44) 1223-336-033; or e-mail: deposit@ccdc.cam.ac.uk. Full details of data collection are provided in Table S1and composition of selected molecular orbitals in Table S2. Packing diagrams showing non-covalent interactions in complexes [Ru(trpy)(pan)]ClO_4 (Fig. S1), [Ru(bpy)(pan)Cl] (Fig. S2) and [Ru$(PPh_3)_2$(pan)Cl] (Fig. S3), and ^{1}H NMR spectrum of [Ru$(pan)_2$] (Fig. S4) have been deposited. Supplementary data associated with this article can be found, in the online version, at doi:10.1016/j.poly.2008.05.023.

References

[1] (a) M. Turki, C. Daniel, Coord. Chem. Rev. 216–217 (2001) 31;
(b) V. Balzani, A. Juris, Coord. Chem. Rev. 211 (2001) 97;
(c) B.Z. Shan, Q. Zhao, N. Goswami, D.M. Eichhom, D.P. Rillema, Coord. Chem. Rev. 211 (2001) 117;
(d) N.A.P. Kane-Maguire, J.F. Wheeler, Coord. Chem. Rev. 211 (2001) 145;
(e) L.N. Ji, X.H. Zou, J.G. Liu, Coord. Chem. Rev. 216–217 (2001) 513;
(f) G. Simonneaux, P. Le Maux, Coord. Chem. Rev. 228 (2002) 43;
(g) H. Yersin, C. Kratzer, Coord. Chem. Rev. 229 (2002) 75;
(h) J.F. Endicott, H.B. Schlegel, M.J. Uddin, D.S. Seniveratne, Coord. Chem. Rev. 229 (2002) 95;
(i) I. Gorelsky, A.B.P. Lever, M. Ebadi, Coord. Chem. Rev. 230 (2002) 97;
(j) F. Hartl, M.P. Aarnts, H.A. Nieuwenhuis, J. van Slageren, Coord. Chem. Rev. 230 (2002) 106;
(k) C.M. Che, J.S. Huang, Coord. Chem. Rev. 231 (2002) 151;
(l) M.J. Clarke, Coord. Chem. Rev. 232 (2002) 69;
(m) E. Tfouni, M. Krieger, B.R. McGarvey, D.W. Franco, Coord. Chem. Rev. 236 (2003) 57;
(n) B. Serli, E. Zangrando, T. Gianferrara, L. Yellowless, E. Alessio, Coord. Chem. Rev. 245 (2003) 73;
(o) M.J. Clarke, Coord. Chem. Rev. 236 (2003) 209;
(p) I. Ando, Coord. Chem. Rev. 248 (2004) 185;
(q) M.A.S. Aquino, Coord. Chem. Rev. 248 (2004) 1025;
(r) R.F. Winter, S. Záli, Coord. Chem. Rev. 248 (2004) 1565;
(s) S. Rigaut, D. Touchard, P.H. Dixneuf, Coord. Chem. Rev. 248 (2004) 1585;
(t) M.K. Nazeeruddin, S.M. Zakeeruddin, J.J. Lagref, P. Liska, P. Comte, C. Barolo, G. Viscardi, K. Schenk, M. Graetzel, Coord. Chem. Rev. 248 (2004) 1317;
(u) L. Spiccia, G.B. Deacon, C.M. Kepert, Coord. Chem. Rev. 248 (2004) 1329;
(v) Y. Saito, T. Azechi, T. Kitamura, Y. Hasegawa, Y. Wada, S. Yanagida, Coord. Chem. Rev. 248 (2004) 1469;
(w) Md.K. Nazeeruddin, C. Klein, P. Liska, M. Grätzel, Coord. Chem. Rev. 249 (2005) 1460.
[2] (a) F. Basuli, S.M. Peng, S. Bhattacharya, Inorg. Chem. 36 (1997) 5645;
(b) F. Basuli, M. Ruf, C.G. Pierpont, S. Bhattacharya, Inorg. Chem. 37 (1998) 6113;
(c) A.K. Das, A. Rueda, L.R. Falvello, S.M. Peng, S. Bhattacharya, Inorg. Chem. 38 (1999) 4365;
(d) A.K. Das, S.M. Peng, S. Bhattacharya, J. Chem. Soc., Dalton Trans. (2000) 181;
(e) F. Basuli, S.M. Peng, S. Bhattacharya, Inorg. Chem. 39 (2000) 1120;
(f) F. Basuli, S.M. Peng, S. Bhattacharya, Inorg. Chem. 40 (2001) 1126;
(g) I. Pal, F. Basuli, T.C.W. Mak, S. Bhattacharya, Angew. Chem., Int. Ed. 40 (2001) 2923;
(h) K. Majumder, R.J. Butcher, S. Bhattacharya, Inorg. Chem. 41 (2002) 4605;
(i) R. Acharyya, S.M. Peng, G.H. Lee, S. Bhattacharya, Inorg. Chem. 42 (2003) 7378;
(j) A. Das, S.M. Peng, G.H. Lee, S. Bhattacharya, New J. Chem. 28 (2004) 712;
(k) S. Nag, P. Gupta, R.J. Butcher, S. Bhattacharya, Inorg. Chem. 43 (2004) 4814;
(l) P.K. Sinha, L.R. Falvello, S. Bhattacharya, Indian J. Chem. 43A (2004) 1846;
(m) P. Gupta, S. Dutta, F. Basuli, S.M. Peng, G.H. Lee, S. Bhattacharya, Inorg. Chem. 45 (2006) 460;
(n) S. Halder, R. Acharyya, S.M. Peng, G.H. Lee, M.G.B. Drew, S. Bhattacharya, Inorg. Chem. 45 (2006) 9654;
(o) S. Nag, R.J. Butcher, S. Bhattacharya, Eur. J. Inorg. Chem. (2007) 1251.
[3] (a) C.D. Hubbard, A.D. Pacheco, J. Inorg. Nucl. Chem. 39 (1977) 1373;
(b) M. Katsura, I. Taira, I. Tasuku, F. Masatoshi, Bull. Chem. Soc. Jpn. 51 (1978) 1743;
(c) K. Shigero, M. Yoshiki, A. Kunihiko, Chem. Lett. (1981) 363;
(d) L.M. Rao, D. Satyanarayana, Indian J. Chem. 22A (1983) 455;
(e) H. Akiharu, F. Shigenobu, T. Motoharu, Bull. Chem. Soc. Jpn. 57 (1984) 1255;
(f) P.M. Drozdzewski, Spectrochim. Acta 44A (1988) 1297;
(g) M.A. Taher, S. Puri, R.K. Bansal, B.K. Puri, Talanta 45 (1997) 411;
(h) S. Nabi, A. Alim, A. Islam, M. Amjad, J. Separ. Sci. 28 (2005) 2463.
[4] (a) R.A. Krause, K. Krause, Inorg. Chem. 19 (1980) 2600;
(b) S. Goswami, A.R. Chakravarty, A. Chakravorty, Inorg. Chem. 20 (1981) 2246;
(c) R.A. Krause, K. Krause, Inorg. Chem. 21 (1982) 1774.
[5] (a) S. Bhattacharya, S.R. Boone, G.A. Fox, C.G. Pierpont, J. Am. Chem. Soc. 112 (1990) 1088;
(b) J. Chakravarty, S. Bhattacharya, Polyhedron 15 (1996) 257;
(c) N.C. Pramanik, S. Bhattacharya, Polyhedron 16 (1997) 1755.
[6] (a) E.P. Benson, J.I. Legg, Inorg. Chem. 20 (1981) 2504;
(b) M.S. El-Shahawi, A.Z. Abu Zuhri, M.M. Kamal, Fresen. J. Anal. Chem. 348 (1994) 730.
[7] (a) I.P. Evans, A. Spencer, G. Wilkinson, J. Chem. Soc., Dalton Trans. (1973) 204;
(b) S. Anderson, K.R. Seddon, J. Chem. Res. (S) (1979) 74;
(c) B.P. Sullivan, J.M. Calvert, T.J. Meyer, Inorg. Chem. 19 (1980) 1404;
(d) T.A. Stephenson, G. Wilkinson, J. Inorg. Nucl. Chem. (1996) 945.
[8] (a) M. Walter, L. Ramaley, Anal. Chem. 45 (1973) 165;
(b) D.T. Sawyer, J.L. Roberts Jr., Experimental Electrochemistry for Chemists, Wiley, New York, 1974. p. 167.
[9] (a) G.M. Sheldrick, SHELXS-97 and SHELXL-97, Fortran Programs for Crystal Structure Solution and Refinement, University of Gottingen, Germany, 1997;
(b) ABSPACK, Oxford Diffraction Ltd., Oxford, UK, 2005.;
(c) CRYSALIS, Oxford Diffraction Ltd., Abingdon, UK, 2006.
[10] (a) A. Seal, S. Ray, Acta Crystallogr., Sect. C 40 (1984) 929;
(b) P. Majumdar, S.M. Peng, S. Goswami, J. Chem. Soc., Dalton Trans. (1998) 1569.
[11] A. Das, S.M. Peng, S. Bhattacharya, Polyhedron 19 (2000) 1227.
[12] (a) H.S. Chow, E.C. Constable, C.E. Housecroft, M. Neuburger, S. Schaffner, Polyhedron 25 (2006) 1831;
(b) M. Fabre, J. Jaud, M. Hliwa, J.P. Launay, J. Bonvoisin, Inorg. Chem. 45 (2006) 9332;
(c) E. Lebon, I.M. Dixon, L. Vendier, A. Igau, P. Sutra, Inorg. Chim. Acta 360 (2007) 1235.
[13] (a) M.F. McGuiggan, L.H. Pingnolet, Inorg. Chem. 21 (1982) 2523;
(b) G.A. Eox, S. Bhattacharya, C.G. Pierpont, Inorg. Chem. 30 (1991) 2895.
[14] (a) C. Mealli, D.M. Proserpio, J. Chem. Edu. 67 (1990) 399;
(b) C. Mealli, D.M. Proserpio, CACAO, version 4.0, Italy, 1994.
[15] (a) C.J. Murphy, J.K. Barton, Methods Enzymol. 226 (1993) 576;
(b) D.S. Sigman, A. Mazumder, D.M. Perrin, Chem. Rev. 93 (1993) 2295;
(c) D.B. Hall, R.E. Holmlin, J.K. Barton, Nature 382 (1996) 731;
(d) P.J. Dandlier, R.E. Holmlin, J.K. Barton, Science 274 (1997) 1465;
(e) F.M. O'Reilly, J.M. Kelly, New J. Chem. 22 (1998) 215;
(f) E. Bernal-Mend~ez, J.S. Sun, F. Gonzalez-Vilchez, M. Leng, New J. Chem. 22 (1998) 1479;
(g) B.A. Jackson, V.Y. Alekseyev, J.K. Barton, Biochemistry 38 (1999) 4655;
(h) L. Mishra, S. Srivastava, A.B. Patel, New J. Chem. 24 (2000) 505.
[16] (a) R.J. Morgan, S. Chatterjee, A.D. Baker, T.C. Strekas, Inorg. Chem. 30 (1991) 2687;
(b) W. Lu, D.A. Vicic, J.K. Barton, Inorg. Chem. 44 (2005) 7970;
(c) L.M. Wu, H.B. Teng, X.B. Ke, W.J. Xu, J.T. Su, S.C. Liang, X.M. Hu, Chem. Biodiv. 4 (2007) 2198.